

## FIELD-ALIGNED CURRENTS BETWEEN CONJUGATE HEMISPHERES

L. Benkevich (*Polar Geophysical Institute, Apatity, Russia*)

W. Lyatsky (*Polar Geophysical Institute, Apatity, Russia, Institute for Space Research, University of Calgary, Calgary, Alberta, Canada T2N 1N4*)

L. L. Cogger (*Institute for Space Research, University of Calgary, Calgary, Alberta, Canada T2N 1N4*)

**Abstract.** Numerical calculations for the generation of interhemispheric field-aligned currents between conjugate ionospheres for different seasons are considered. The currents are produced because of the difference in the ionospheric conductivity in the dark and sunlit conjugate hemispheres, and they are a result of redistribution of original 3D currents for the case of different ionospheric conductivity distribution in both hemispheres. Interhemispheric currents and related patterns for electric potential distribution are computed for reasonable models of the ionospheric conductivity. The currents are attached to the terminator position, and they close a part of ionospheric currents generated in the sunlit high-latitude ionosphere of the summer hemisphere, through the conjugate ionosphere of the other hemisphere. Thus, interhemispheric currents in the winter ionosphere are generated mainly by sources in the summer hemisphere.

### 1. Introduction

The interhemispheric currents can be generated by symmetric sources in both hemispheres when there is a difference between the ionospheric conductivity in the northern and southern hemispheres which is especially pronounced for summer/winter conditions. The role of the interhemispheric conductivity asymmetry in the generation of interhemispheric currents was discussed by *Lu et al.* [1994] and *Gasda and Richmond* [1998]. Such interhemispheric currents should be concentrated on a boundary where the gradient of the conductivity variation is the greatest, for instance, at the terminator. The appearance of the polarization electric field and field-aligned currents at the terminator has been studied earlier by *Atkinson and Hutchinson* [1978] and *Maltsev and Lyatsky* [1982b]. The total magnitude of interhemispheric currents in this case is approximately equal to that of ionospheric currents entering a terminator position, and can be roughly estimated as  $I_{\parallel} = x\Sigma_H E$  where  $\Sigma_H$  is the Hall ionospheric conductivity,  $E$  is the ionospheric electric field along the terminator, and  $x$  is the distance between sources of these currents. For typical magnitudes of  $\Sigma_H$  in the winter sunlit ionosphere equatorward the terminator about  $6 S$  [*Hardy et al.*, 1987],  $E = 50 mV/m$ , and  $x = 2000 km$ , we obtain  $I_{\parallel} = 3 \times 10^5 A$ , which is comparable with the magnitude of total  $RI$  field-aligned currents of about  $10^6 A$  [*Potemra*, 1994] and is several times more than that provided for neutral winds [*Richmond and Roble*, 1987].

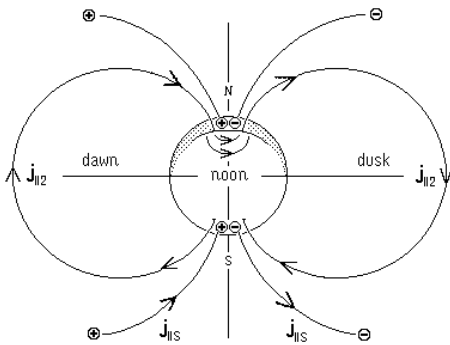


Figure 1. Generation of interhemispheric FACs for winter conditions in the northern hemisphere

The aim of the present paper is to examine interhemispheric field-aligned currents between conjugate high-latitude ionospheres due to the asymmetry of the ionospheric conductivity between conjugate ionospheres during summer/winter conditions. We consider the generation of interhemispheric currents and calculate resulting patterns for the ionospheric ones using a simple model of the ionospheric conductivity distribution. The interhemispheric currents appear at the magnetic field lines going out of the terminator. Some expected effects of these interhemispheric currents in auroral and magnetic events are discussed.

### 2. Generation of interhemispheric currents during winter-summer conditions

Figure 1 shows the dayside ionosphere as seen from a point lying at the noon meridian in the equatorial plane for winter conditions in the northern hemisphere. During winter months, a part of the dayside ionosphere in the northern hemisphere is dark (in the figure it is shown by the dotted area). This is a region of small ionospheric conductivity.

Original field-aligned currents flowing into the dawn sectors and out of the dusk sectors of the southern (S) high-latitude ionosphere are shown by  $j_{\parallel S0}$  and  $j_{\parallel N0}$ . These currents support in the ionosphere positive (+) and negative (-) electric charges. The field-aligned currents close ionospheric currents. Because of small magnitude of the conductivity in the dark northern ionosphere, no significant ionospheric currents occur there. However, since the northern and southern ionospheres are connected by highly-conductive magnetic field-lines, a part of the ionospheric currents from the southern hemisphere closes the interhemispheric field-aligned currents, which in their turn close the ionospheric currents in the sunlit northern lower-latitude ionosphere (Region 2 in Figure 2). These interhemispheric currents denoted in Figure 1 and 2 as  $j_{\parallel 2}$  are attached to a strong gradient of the ionospheric conductivity in the northern ionosphere, which corresponds to the terminator position.

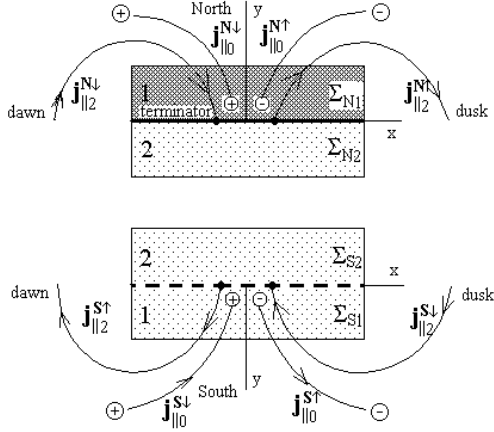


Figure 2. The model adopted to expedite the problem solution. The dashed line is the terminator projection.

reality they are distributed in some region around the terminator. In order to derive interhemispheric field-aligned currents, we must first derive the potential distribution. Because of high conductivity along field lines, the electric potential distribution in the region of closed magnetic lines is the same in the both ionospheres. We can project along field lines the region of closed field lines of the northern ionosphere onto the southern ionosphere. Since conjugate points have the same potential, the potential distribution in the resulting overlapping model remains the same, but such superposition allows us to eliminate the interhemispheric field-aligned currents. The resulting overlapping ionospheric model is shown in Figure 3. The conductivity components in the north region being  $\Sigma_P^N$  and  $\Sigma_H^N$ , and in the south region  $\Sigma_P^S$  and  $\Sigma_H^S$ , these components in the overlapping region are  $\Sigma_P = \Sigma_P^N + \Sigma_P^S$  and  $\Sigma_H = \Sigma_H^N + \Sigma_H^S$ . The potential distribution in the overlapping model can be obtained as a solution to some Poisson equation. To derive the equation, we associate the incident current  $\mathbf{j}_{||0} = \mathbf{j}_{||N0} + \mathbf{j}_{||S0}$  with the sheet ionospheric currents  $\mathbf{J}$ :

$$\nabla \cdot \mathbf{J} = \mathbf{e}_z \cdot \mathbf{j}_{||0}, \quad (4)$$

where  $\mathbf{e}_z$  is a Z directed unit vector. According to the Ohm law,

$$\mathbf{J} = \mathfrak{E} \mathbf{E} = -\mathfrak{E} \nabla \varphi, \quad (5)$$

where  $\mathfrak{E}$  is the height-integrated conductivity tensor,

$$\mathfrak{E} = \begin{pmatrix} \Sigma_P & \Sigma_H \\ -\Sigma_H & \Sigma_P \end{pmatrix}, \text{ and } \varphi = \varphi(x, y) \text{ is the sheet electric potential function}$$

to be found. Substituting (2) into (1) yields the Poisson equation

$$\nabla \cdot (\mathfrak{E} \nabla \varphi) = -\mathbf{e}_z \cdot \mathbf{j}_{||0}, \quad (6)$$

or, in more detail:

$$\Sigma_P \left( \frac{\partial^2 \varphi}{\partial x^2} + \frac{\partial^2 \varphi}{\partial y^2} \right) + \left( \frac{\partial \Sigma_P}{\partial x} - \frac{\partial \Sigma_H}{\partial y} \right) \frac{\partial \varphi}{\partial x} + \left( \frac{\partial \Sigma_H}{\partial x} + \frac{\partial \Sigma_P}{\partial y} \right) \frac{\partial \varphi}{\partial y} = -\mathbf{e}_z \cdot \mathbf{j}_{||0}. \quad (7)$$

Figure 4 shows a typical potential distribution.

In their turn, the field aligned currents between the hemispheres can be derived by applying the differential operator in the left hand side of the Poisson equation (7) to the obtained potential. However, for this once instead of the total conductivity components,  $\Sigma_P$  and  $\Sigma_H$ , one should use their either north,  $\Sigma_P^N, \Sigma_H^N$ , or south,  $\Sigma_P^S, \Sigma_H^S$  parts. Thus, the entire FAC system incident on the northern ionospheric region (including a fraction of the original FAC  $\mathbf{j}_{||0}$ ), is calculated as

$$\mathbf{e}_z \cdot \mathbf{j}_{||}^N = \Sigma_P^N \left( \frac{\partial^2 \varphi}{\partial x^2} + \frac{\partial^2 \varphi}{\partial y^2} \right) + \left( \frac{\partial \Sigma_P^N}{\partial x} - \frac{\partial \Sigma_H^N}{\partial y} \right) \frac{\partial \varphi}{\partial x} + \left( \frac{\partial \Sigma_H^N}{\partial x} + \frac{\partial \Sigma_P^N}{\partial y} \right) \frac{\partial \varphi}{\partial y}. \quad (8)$$

### 3. Model of conductivity and the problem solution method

Figure 2 shows the model of ionosphere used to solve the problem in two hemispheres. The model of ionospheric conductivity distribution suggested by Robinson and Vondrak [1984] was adopted:

$$\Sigma_P = 1 + 0.88(S_a \cos \chi)^{0.5}, \quad (S) \quad (1)$$

$$\Sigma_H = 1 + 1.5(S_a \cos \chi)^{0.5}. \quad (S) \quad (2)$$

where  $S_a$  is the solar power flux at 10.7 cm (in units of  $10^{-22} \text{ W/m}^2$ ) and  $\chi$  is the zenith angle. Over a year,  $\chi$  undergoes one period of harmonic variation:

$$\chi = 23.45 \cos(2\pi(d+10)/365)^\circ, \quad (3)$$

where  $d$  is a day number within a year,  $d = 1 \dots 365$ . Over a solar cycle, the monthly average of the solar flux  $S_a$  varies from about 60 at solar minimum to 240 at solar maximum [Hardy et al., 1987].

Figure 2 also shows locations of the initial field-aligned currents,  $\mathbf{j}_{||S0}$  and  $\mathbf{j}_{||N0}$  which are assumed to be poleward of the terminator. Interhemispheric currents arising around the terminator are shown as  $\mathbf{j}_{||2}$ . Although they are depicted only on the terminator position, in

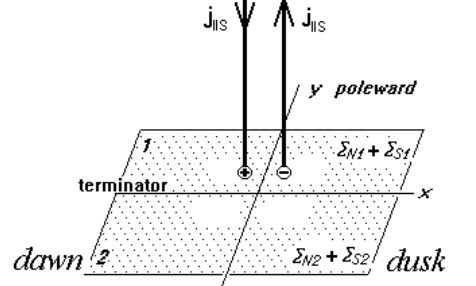


Figure 3. The overlapping model. No interhemispheric FACs, only sources

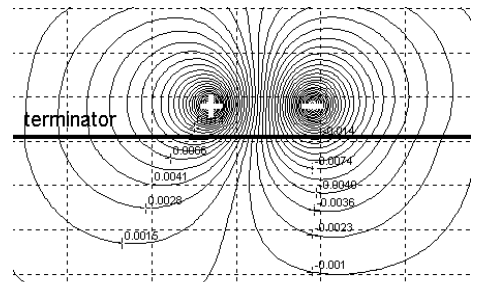


Figure 4. The calculated electric potential distribution for the north hemisphere.

#### 4. Results of calculations

The experiments have been conducted on grid numeric domains. The grids were located at the conjugate regions of the ionosphere and at the high latitudes, so that the terminator crossed the north domain in the middle. Daily solar energy flux at 10.3 cm,  $S_a$ , affects FACs value, too, so it was used as a parameter. Due to linearity of the problem the resulting currents and potential patterns are linearly scalable, so all the simulation was held in relative units. There were two distributed magnetospheric voltage sources producing two incident current filaments, positive,  $\mathbf{j}_{\parallel 0}^{\downarrow}$ , and negative,  $\mathbf{j}_{\parallel 0}^{\uparrow}$ . For  $\mathbf{j}_{\parallel 0}^{\downarrow}$  and  $\mathbf{j}_{\parallel 0}^{\uparrow}$  a simple, smooth 2-D distribution was selected,  $\mathbf{j}_{\parallel 0}^{\downarrow} = 0.079589 \exp(-0.25(x^2 + y^2))$  and  $\mathbf{j}_{\parallel 0}^{\uparrow} = -\mathbf{j}_{\parallel 0}^{\downarrow}$ , with a unit integral flow each.

##### 4.1. Electric potential distribution

The distribution of the electric potential and field-aligned currents are obtained by a numerical solution of equation (7). The potential distribution shown in Figure 4 is the same both for the southern and northern hemispheres (if viewed from the northern pole) because of the highly-conductive magnetic field lines. A kink of the potential contours on the terminator implies the appearance there of electric charges, which are associated with interhemispheric field-aligned currents. We note that the potential distribution in Figure 4 may be referred to stationary sources of the magnetospheric convection as well as to non-stationary events such as the travelling convection vortices if their sources are located poleward of the terminator position.

##### 4.2. Field-aligned currents

The field-aligned currents emerging at the terminator were also obtained numerically by applying operators (7) to the potential distribution. Figure 5 shows a typical FACs distribution. Like the original FACs, these secondary currents flowing between N and S hemispheres along the closed geomagnetic field lines also form two filaments: a positive one,  $\mathbf{j}_{\parallel 2}^{\downarrow}$ , and a negative one,  $\mathbf{j}_{\parallel 2}^{\uparrow}$  (if viewed from the north region). However, unlike the original FACs whose magnitude depends on the ionospheric conductance, the secondary ones at every pair of conjugate points have equal absolute values and opposite signs. These currents only flow above sunlit regions. Their magnitudes gain maximum (or minimum) at the terminator and subside equatorward. It should be noted that the extremums of  $\mathbf{j}_{\parallel 2}^{\downarrow}$  and  $\mathbf{j}_{\parallel 2}^{\uparrow}$  are substantially displaced eastward. The effect should be related to the Hall conductivity. If there were only the Pedersen conductance, the maximum of the interhemispheric FACs would be located immediately under the original FACs footprint, i.e. on the perpendicular to the terminator. The convection, however, with its circular current round the FACs footprint contributes to the interhemispheric currents at a distance from the perpendicular, forming some eastward shift of  $\mathbf{j}_{\parallel 2}^{\downarrow}$  and  $\mathbf{j}_{\parallel 2}^{\uparrow}$  extremums.

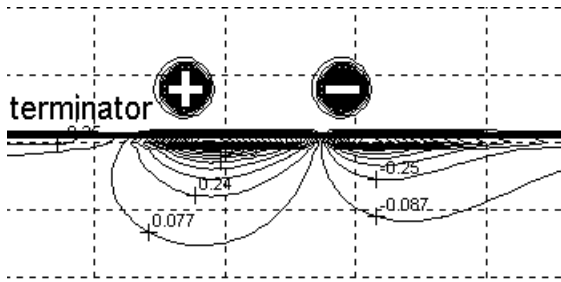


Figure 5. Contour lines of the secondary FACs emerged on the terminator.

##### 4.3. Dependence of field-aligned current magnitude on distance between sources and their location with respect to the terminator

In order to find out what fraction of the total southern FACs branch into the secondary ones we conducted a series of experiments under the following conditions. The terrene axis inclination angle,  $\alpha$ , is  $23.45^\circ$  and the highest terminator latitude,  $\chi$ , is  $66.55^\circ$ , which corresponds to the vernal equinox. We chose the distance between the primary currents sources  $a=330\text{km}$  (equivalent to about  $3^\circ$  along meridian), and varied  $b$ , the distance between a source and the terminator. The dependence of  $\delta I_2^{\downarrow N, \%}$ , the quota of inflowing secondary currents relative to inflowing original currents, on the ratio  $b/a$  has been plotted and presented in Figure 6. The two curves are drawn for minimum and maximum of the solar activity. Both of the curves have a maximum at approximately  $b/a = 5.4$ . Presumably it is caused by superposition of the Hall currents contributions to the secondary FACs. When the sources are close enough to each other, their Hall currents sum and form maximum near the terminator. When the sources are too close, the effect is weaker because a considerable part of the sheet current flows immediately from (+) source into the (-) one. When the sources are too far from each other, their Hall currents do not form a pronounced maximum, and again a lesser fraction of the original currents is transferred into the secondary ones.

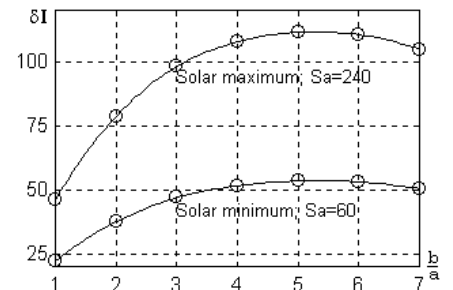


Figure 6. Dependence of the secondary FACs magnitude on distance between the sources.

#### 5. Discussion and conclusions

The asymmetry in the ionospheric conductivity in the northern and southern hemispheres during winter/ summer conditions leads thus to the appearance of interhemispheric field-aligned currents on magnetic field lines going out of

the terminator position. The total magnitude of these currents is close to one half of that of ionospheric currents crossing the terminator projection in the sunlit ionosphere.

Another interesting consequence of the model considered above is that the upward directed interhemispheric currents may lead to the generation of auroras [Lyons, 1981; Kozlovsky and Lyatsky, 1994; Stenbaek-Nielsen and Otto, 1997] near the terminator.

The observations of the auroras around the terminator might be possible from the satellite based UV images. The generation of auroras on magnetic field lines going out from the terminator is a prediction based on our study.

The main results of the work can be formulated as follows:

1. Because of the difference in magnitudes of the ionospheric conductivity in the high-latitude ionospheres of the northern and southern hemispheres during summer/winter conditions, interhemispheric field-aligned currents appear along the magnetic field lines going out from the terminator position

2. FACs and ionospheric currents in the dayside winter ionosphere are generated mainly by sources in the sunlit summer hemisphere. The FACs are attached to the terminator position. The centres of the ionospheric convection vortices are attached to sources of the electric field which may be located several degrees of latitude polewards of the terminator.

3. One more interesting consequence of interhemispheric currents is that no correlation but rather anti-correlation between auroral and magnetic events associated with these currents must occur in the opposite hemispheres.

*Acknowledgements.* We are grateful to D. Knudsen and B. Jackel for the useful discussion. This research was partially funded by the Natural Sciences and Engineering Research Council of Canada and it was also supported by the Russian Foundation for Basic Researches (grant No 97-05-65894).

### **References**

- Atkinson, G., and D. Hatchinson, Effect of day-night ionospheric conductivity on polar cap convective flow, *J. Geophys. Res.*, *83*, 725, 1978.
- Benkevich L. and W. Lyatsky, An analytical model for non-conjugation of the equivalent currents in the dayside high-latitude ionosphere, Proceedings of the 21<sup>st</sup> Annual Seminar "Physics of Auroral Phenomena", Apatity, 1998.
- Gasda, S., and A. D. Richmond, Longitudinal and interhemispheric variations of auroral ionospheric electrodynamics in a realistic geomagnetic field, *J. Geophys. Res.*, *103*, 4011, 1998.
- Hardy, D. A., M. S. Gussenhoven, and R. Raistrick, Statistical and functional representations of the pattern of auroral energy flux, number flux, and conductivity, *J. Geophys. Res.*, *92*, 12,275, 1987.
- Kozlovsky, A. E., and W. B. Lyatsky, Instability of the magnetosphere-ionosphere convection and formation of auroral arcs, *Ann. Geophys.*, *12*, 636-641, 1994.
- Lu, G., et al., Interhemispheric asymmetry of the high-latitude ionospheric convection pattern, *J. Geophys. Res.*, *99*, 6491, 1994.
- Lyons, L. R., Discrete auroras as the direct result of an inferred high-latitude generating potential distribution, *J. Geophys. Res.*, *86*, 1, 1981.
- Maltsev, Y. P., and W. B. Lyatsky, Effect of the terminator on electric field and field-aligned currents, *Kosmicheskie Issledovaniya* (in Russian), *20*, 304-308, 1982.
- Potemra, T. A., Sources of large-scale Birkeland currents, in *Physical Signatures of Magnetospheric Boundary Layer Processes*, Edited by J. A. Holtet and A. Egeland, p.3, Kluwer Academic Publishers, 1994.
- Richmond, A. D., and R. G. Roble, Electrodynamics effects of thermospheric winds from NCAR thermospheric general circulation model, *J. Geophys. Res.*, *92*, 12,365-12,376, 1987.
- Stenbaek-Nielsen, H. C., and A. Otto, Conjugate auroras and the interplanetary magnetic field, *J. Geophys. Res.*, *102*, 2223-2232, 1997.